Bulk Superconducting Phase with a Full Energy Gap in the Doped Topological Insulator $Cu_xBi_2Se_3$

M. Kriener, Kouji Segawa, Zhi Ren, Satoshi Sasaki, and Yoichi Ando
Institute of Scientific and Industrial Research, Osaka University, Osaka 567-0047, Japan
(Received 1 December 2010; published 23 March 2011)

The superconductivity recently found in the doped topological insulator $Cu_xBi_2Se_3$ offers a great opportunity to search for a topological superconductor. We have successfully prepared a single-crystal sample with a large shielding fraction and measured the specific-heat anomaly associated with the superconductivity. The temperature dependence of the specific heat suggests a fully gapped, strong-coupling superconducting state, but the BCS theory is not in full agreement with the data, which hints at a possible unconventional pairing in $Cu_xBi_2Se_3$. Also, the evaluated effective mass of $2.6m_e$ (m_e is the free electron mass) points to a large mass enhancement in this material.

DOI: 10.1103/PhysRevLett.106.127004 PACS numbers: 74.25.Bt, 74.25.Op, 74.62.Dh, 74.70.Ad

In the past two years, the three-dimensional (3D) topological insulator (TI) has been attracting a lot of interest as a new state of matter [1–3]. It is characterized by the existence of a gapless surface state that emerges because of the nontrivial Z_2 topology of the insulating bulk state and is protected against backscattering by time-reversal symmetry. The discovery of the 3D TI stimulated the search for a superconducting (SC) analogue, a time-reversal-invariant topological superconductor [4–9], which is characterized by a fully gapped, odd-parity pairing state that leads to the emergence of gapless Majorana surface states. Such a SC phase has implications on topological quantum computing [4,10–12] because of the non-Abelian Majorana bound state expected to appear in the vortex core. However, a concrete example of such a topological superconductor is currently unknown.

In this context, the superconductivity recently found [13] in $Cu_xBi_2Se_3$ is very interesting. Bi_2Se_3 is a "second-generation" TI that has a relatively large (~ 0.3 eV) band gap and a simple surface-state structure [14,15]. Surprisingly, when Cu is introduced to this system with the nominal formula $Cu_xBi_2Se_3$, superconductivity with a maximum transition temperature T_c of 3.8 K was observed for the doping range $0.10 \leq x \leq 0.30$, even though the bulk carrier density n was only $\sim 10^{20}$ cm^{-3} [13]. Note that this T_c is uncharacteristically high for such a low n [16]. Furthermore, the topological surface state was found to be well separated from the doped bulk conduction band in $Cu_xBi_2Se_3$ [17]. So far, apparent SC shielding fractions of only up to 20% have been achieved and the resistivity always remained finite [13,17], leaving some doubt about the bulk nature of the superconductivity in this system. Nonetheless, if this superconductivity is indeed a bulk property of carrier-doped Bi_2Se_3, it has a profound implication on the search of topological superconductors, because (i) it is a potential candidate [18] to realize a 3D topological superconductor, and (ii) if its bulk turns out to be an ordinary s-wave superconductor, the topological surface state may turn into a 2D topological superconductor as a result of a SC proximity effect [4]. Therefore, it is important to confirm whether the superconductivity is really occurring in the bulk of $Cu_xBi_2Se_3$ and, if so, to elucidate the fundamental nature of its SC state.

Bi_2Se_3 has a layered crystal structure ($R\bar{3}m$, space group 166) consisting of stacked Se-Bi-Se-Bi-Se quintuples that are only weakly van der Waals bonded to each other. We call the rhombohedral [111] direction the c axis and the (111) plane the ab plane. When Cu is introduced into Bi_2Se_3, it may either intercalate as Cu^{1+} into the van der Waals gaps and act as a donor, or replace Bi as a substitutional impurity and act as an acceptor [19]; hence, Cu is an ambipolar dopant [20,21]. The nominal formula of $Cu_xBi_2Se_3$ suggests that most Cu atoms in this SC material occupy the intercalation sites; however, the reported carrier density of $\sim 10^{20}$ cm^{-3} [13] corresponds to only $\sim 1\%$ of electron doping, which is much smaller than that expected from the x value. This discrepancy suggests either that most of the intercalated Cu ions remain inactive as donors, or that substitution of Bi with Cu also occurs in this material and it almost compensates the electrons doped by the intercalated Cu. Partly related to such an uncontrollability of the Cu atoms in $Cu_xBi_2Se_3$, the quality of the SC samples has been poor as mentioned above, and improvements in the sample quality are indispensable for a solid understanding of the SC state in this material.

In this Letter, we report a comprehensive study of the basic SC properties of a Cu-intercalated Bi_2Se_3 single crystal by means of resistivity, magnetization, and specific-heat measurements. We observed zero resistivity in this material and a specific-heat jump at the SC transition. The apparent shielding fraction of our sample exceeds 40%, and the specific-heat data confirm the bulk nature of the superconductivity. Most importantly, the temperature dependence of the specific heat suggests a fully gapped, strong-coupling SC state, but the data do

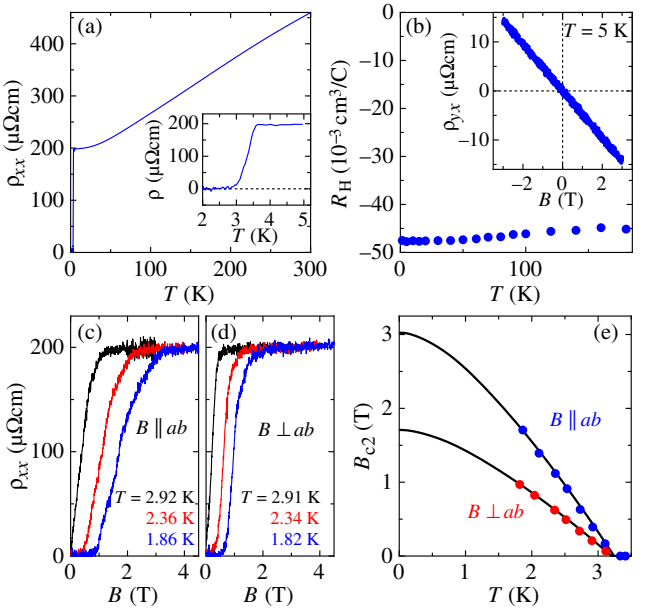

FIG. 1 (color online). (a) $\rho_{xx}(T)$ data of the $Cu_{0.29}Bi_2Se_3$ sample. (b) Temperature dependence of R_H; inset shows the $\rho_{yx}(B)$ data at 5 K. (c),(d) $\rho_{xx}(B)$ data for $B \parallel ab$ and $B \perp ab$, respectively. (e) B_{c2} vs T phase diagram determined from the midpoint in $\rho_{xx}(B)$ at various temperatures; solid lines show the WHH behavior. The midpoint definition for B_{c2} gives $T_c = 3.2$ K consistent with the $M(T)$ data.

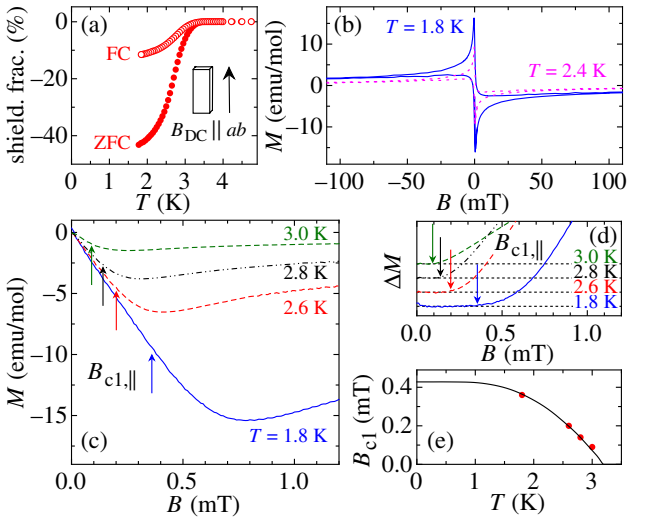

FIG. 2 (color online). (a) Temperature dependence of the apparent shielding fraction of $Cu_{0.29}Bi_2Se_3$ measured in $B = 0.2$ mT $\parallel ab$. (b) $M(B)$ curves at 1.8 and 2.4 K after subtracting the diamagnetic background. (c) Initial $M(B)$ behavior after ZFC to various temperatures. Arrows mark the position of $B_{c1,\parallel}$. Note the very small magnetic-field scale. (d) Plots of $\Delta M \equiv M - aB$, where a is the initial slope, and the determination of $B_{c1,\parallel}$ shown by arrows. (e) $B_{c1,\parallel}$ vs T phase diagram; the solid line is a fit within the local dirty limit.

not fully agree with the strong-coupling BCS calculation. This suggests that the pairing symmetry may not be a simple isotropic s wave. Furthermore, the effective mass is found to be $2.6m_e$ (m_e is the free electron mass), suggesting a change in the bulk band curvature.

5 Single crystals of Bi_2Se_3 were grown by melting stoichiometric amounts of elemental shots of Bi (99.9999%) and Se (99.999%) in sealed evacuated quartz glass tubes at 800 °C for 48 h, followed by a slow cooling to 550 °C over 48 h and keeping at that temperature for 24 h. The crystals were cleaved and cut into rectangular pieces, and then the Cu intercalation was done by an electrochemical technique under an inert atmosphere inside a glove box, using CuI reagent in CH_3CN solvent. The sample was wound with a Cu wire, and a Cu stick was used as a counter and reference electrode. The current was fixed at typically 10 μA. The concentration of intercalated Cu was determined from the weight change before and after the intercalation process, and the sample was briefly annealed afterward. The particular sample used in the present study was 3.9×1.6 mm^2 in the ab plane with a thickness of 0.40 mm, and its Cu concentration was $x = 0.29$. In fact, by employing electrochemical intercalation, we found that samples with x of up to $\sim$0.5 become superconducting; the precise phase diagram is currently under investigation.

6 The magnetization data were measured with a commercial SQUID magnetometer (Quantum Design, MPMS). The resistivity ρ_{xx} and the Hall resistivity ρ_{yx} were measured by a standard six-probe technique, where the electrical current was applied in the ab plane. The specific-heat c_p data were taken by a relaxation-time method using a commercial system (Quantum Design, PPMS); the addenda signal was measured before mounting the sample and was duly subtracted from the measured signal. The c_p measurement was done in zero field (for the SC state) and in 2 T applied along the c axis (for the normal state), and the change of the addenda signal between the two was found to be negligible.

7 Figure 1 shows the results of the transport measurements. In zero field, the onset of the SC transition occurs at 3.6 K and zero resistivity was observed at 2.8 K [Fig. 1(a)]. From the magnetic-field (B) dependence of ρ_{xx} [Figs. 1(c) and 1(d)], the upper critical field $B_{c2}(T)$ defined as the midpoint of the resistivity transition [22] is obtained for the two principal field directions [Fig. 1(e)], and the extrapolation to 0 K using the Werthamer-Helfand-Hohenberg (WHH) theory gives $B_{c2,\perp}(0)$ and $B_{c2,\parallel}(0)$ (perpendicular and parallel to the ab plane) of 1.71 and 3.02 T, respectively [Fig. 1(e)]. As shown in the inset of Fig. 1(b), ρ_{yx} is completely linear in B, suggesting the dominance of only one type of bulk carrier. The Hall coefficient R_H was found to be only weakly temperature dependent [Fig. 1(b)] and gives the electron density $n = 1.3 \times 10^{20}$ cm^{-3}.

8 Figure 2 summarizes the magnetization M measurements. To minimize the effect of the demagnetization factor, those measurements were made for $B \parallel ab$

[see the sketch in Fig. 2(a)]. The temperature dependence of the diamagnetic shielding fraction for the zero-field-cooled (ZFC) and field-cooled (FC) measurements are shown in Fig. 2(a), where the onset of the Meissner signal occurs at $T_c = 3.2$ K and the apparent shielding fraction reaches 43% at 1.8 K [23]. Note that this Meissner T_c corresponds to the midpoint of the resistivity transition.

9 Magnetization $M(B)$ curves are shown in Figs. 2(b) and 2(c); each data set was obtained after cooling to its respective temperature from above T_c in zero field, and the background diamagnetism, which can be easily determined at $B > B_{c2,\|}$, is subtracted from the data. As already noted by Hor *et al.* [13], the lower critical field B_{c1} is very small: using the deviation of the $M(B)$ curve from its initial linear behavior as a measure of $B_{c1,\|}$ [Fig. 2(d)], we obtained the $B_{c1,\|}(T)$ data shown in Fig. 2(e). To determine the 0-K limit, we used $B_{c1} \propto 1/\lambda_{\rm eff}^2 \propto [(\Delta(T)/\Delta(0))\tanh(\Delta(T)/2k_BT)]$ for the local dirty limit [25] to fit the extracted data points ($\lambda_{\rm eff}$ is the effective penetration depth and Δ is the SC gap [26]), and obtained $B_{c1,\|}^{\rm app}(0) = 0.43$ mT. For the quantitative analysis discussed later, this apparent value was corrected for the demagnetization effect, though it is small for $B \| ab$: using the approximation given for the slab geometry [24], we obtain $B_{c1,\|}(0) = B_{c1,\|}^{\rm app}(0)/\tanh\sqrt{0.36b/a} = 0.45$ mT, where $b/a = 3.9/0.40$ in our case. Note that the flux pinning in the present system is weak as evidenced by the low irreversibility field of $\sim$0.1 T at 1.8 K [Fig. 2(b)].

10 The temperature dependence of c_p is shown in Fig. 3(a) as c_p/T vs T for the SC state ($B = 0$ T) and the normal state achieved by applying $B \perp ab$ of 2 T ($> B_{c2,\perp}$). As shown by the dotted line in Fig. 3(a), a conventional Debye fit to the normal-state data below 4 K using $c_p = c_{\rm el} + c_{\rm ph} = \gamma_n T + A_3T^3 + A_5T^5$, with the normal-state specific-heat coefficient γ_n and the coefficients of the phononic contribution A_3 and A_5, yields a good description of the data. The obtained parameters are $\gamma_n = 1.95$ mJ/mol K^2, $A_3 = 2.22$ mJ/mol K^4 [27], and $A_5 = 0.05$ mJ/mol K^6. Subtracting the phononic contribution from the zero-field data gives the electronic specific heat $c_{\rm el}$ in the SC state plotted in Fig. 3(b), revealing a clear jump around T_c. This provides compelling evidence for bulk superconductivity in $Cu_xBi_2Se_3$. In passing, we note that our c_p data in 2 T do not exhibit any Schottky anomaly related to electron spins, suggesting that there is no local moment possibly associated with Cu^{2+} ions.

11 From the above results, one can estimate various basic parameters. Assuming a single spherical Fermi surface, one obtains the Fermi wave number $k_F = (3\pi^2 n)^{1/3} = 1.6$ nm^{-1}. The effective mass m^* is evaluated as $m^* = (3\hbar^2\gamma_n)/(V_{\rm mol}k_B^2k_F) = 2.6m_e$, with the molar volume of Bi_2Se_3 $V_{\rm mol} \approx 85$ cm^3/mol. Note that the effective mass of pristine Bi_2Se_3 is $\sim 0.2m_e$ [28], so there is an order-of-magnitude mass enhancement in $Cu_xBi_2Se_3$ [29]. Since

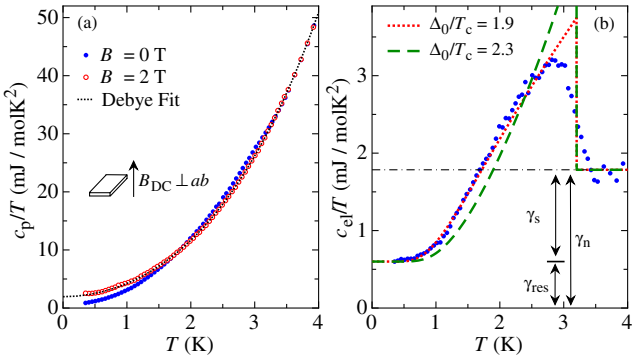

FIG. 3 (color online). (a) $c_p(T)/T$ data measured in 0 and 2 T applied along the c axis; the latter represent the normal-state behavior. The dashed line is a fit to the 2-T data using the standard Debye formula. (b) Electronic term $c_{\rm el}/T$ in 0 T obtained after subtracting the phonon term determined in 2 T. The dotted line shows the calculated $c_{\rm el}/T$ curve given by strong-coupling BCS theory with $\alpha = 1.9$; the dashed line is the BCS curve for $\alpha = 2.3$, which is obtained from B_c, N_0, and T_c. The horizontal dash-dotted line denotes the value of γ_n, and its breakdown to γ_s and $\gamma_{\rm res}$ is indicated.

electron correlations are weak in Bi_2Se_3, the origin of this enhancement is most likely a change in the band curvature near the Fermi level. From $B_{c2,\perp} = 1.71$ T, the coherence length $\xi_{ab} = \sqrt{\Phi_0/(2\pi B_{c2,\perp})} = 13.9$ nm is obtained, while from $B_{c2,\|}$ we use $\xi_{ab}\xi_c = \Phi_0/(2\pi B_{c2,\|})$ and obtain $\xi_c = 7.9$ nm. Since we have the B_{c1} value only for $B \| ab$, we define the effective GL parameter $\kappa_{ab} \equiv \sqrt{\lambda_{ab}\lambda_c/\xi_{ab}\xi_c}$ and use $B_{c1,\|} = \Phi_0 \ln\kappa_{ab}/(4\pi\lambda_{ab}\lambda_c)$ together with $B_{c2,\|}/B_{c1,\|} = 2\kappa_{ab}^2/\ln\kappa_{ab}$ [30] to obtain $\kappa_{ab} \approx 128$. We then obtain the thermodynamic critical field $B_c = \sqrt{B_{c1,\|}B_{c2,\|}/\ln\kappa_{ab}} = 16.7$ mT.

12 To analyze $c_{\rm el}/T$ in the SC state shown in Fig. 3(b), we tried to fit the BCS-type temperature dependence to the data. Since the simple weak-coupling BCS model does not describe the $c_{\rm el}/T$ data (not shown), we use the modified BCS model applicable to strong-coupling superconductors as proposed in Ref. [31], where it is called "α model" with $\alpha = \Delta_0/T_c$ and Δ_0 is the SC gap size at 0 K. We note that strong coupling means $\alpha > \alpha_{\rm BCS} = 1.764$, and that this model still assumes a fully gapped isotropic s-wave pairing. Using the theoretical curve $c_{\rm el}^{\rm BCS}$ of the α model [31], we tried to reproduce the experimental data with $c_{\rm el}(T)/T = \gamma_{\rm res} + c_{\rm el}^{\rm BCS}(T)/T$. Note that the parameter $\gamma_{\rm res}$ is necessary for describing the contribution of the non-SC part of the sample [32]; also, the theoretical term $c_{\rm el}^{\rm BCS}/T$ is set to yield γ_s ($= \gamma_n - \gamma_{\rm res}$) at $T > T_c$.

13 It turned out that with $\alpha = 1.9$, $\gamma_{\rm res} = 0.6$ mJ/mol K^2, and $\gamma_s = 1.185$ mJ/mol K^2, the experimental data are reasonably well reproduced and the entropy balance is satisfied, as shown in Fig. 3(b) by the dotted line and the dash-dotted line [33]. This result strongly suggests that the SC state of $Cu_xBi_2Se_3$ is fully gapped. The resulting

γ_n ($= \gamma_{\rm res} + \gamma_s$) value of 1.785 mJ/mol K^2 slightly deviates from the γ_n value estimated from the Debye fit to the normal-state data in 2 T, 1.95 mJ/mol K^2. This slight difference ($\sim 9\%$) might be the result of a possible field dependence of γ_n, which has to be clarified in future studies.

14 To gain further insight into the nature of the SC state in $Cu_xBi_2Se_3$, we examine the implication of the obtained γ_s value: The density of states (DOS) N_0 is calculated from γ_s via $N_0 = \gamma_s/(\pi^2 k_B^2/3) = 1.51$ states/eV per unit cell, which is large for a low-carrier-density system and is in accord with the "high" T_c. This value allows us to calculate Δ_0 through the expression for the SC condensation energy $\frac{1}{2}N_0\Delta_0^2 = (1/2\mu_0)B_c^2$. With $B_c \approx 16.7$ mT already calculated, we obtain $\Delta_0 = 7.3$ K which gives the coupling strength $\alpha = \Delta_0/T_c = 2.3$. This exceeds the BCS value of 1.764 and hence $Cu_xBi_2Se_3$ is a strong-coupling superconductor, as was already inferred in our analysis of the $c_{\rm el}/T$ data. More importantly, the α value of 2.3 obtained from γ_s is too large to explain the $c_{\rm el}(T)$ data within the strong-coupling BCS theory: as shown in Fig. 3(b) with the dashed line, the expected BCS curve for $\alpha = 2.3$ does not agree with the data at all. This probably means that the actual temperature dependence of Δ in $Cu_xBi_2Se_3$ is different from that of the BCS theory, which suggests that the pairing symmetry may not be the simple isotropic s wave. Obviously, a direct measurement of Δ_0 and $\Delta(T)$ is strongly called for. On the other hand, the low-temperature behavior of $c_{\rm el}(T)$ robustly indicates the absence of nodes and points to a fully gapped state. It will be interesting to see if the fully gapped, time-reversal-invariant p-wave state proposed for $Cu_xBi_2Se_3$ [18] would provide a satisfactory explanation of our data.

15 In summary, we report a comprehensive study of the superconductivity in $Cu_xBi_2Se_3$ by means of resistivity, magnetization, and specific-heat measurements on a single crystal with $x = 0.29$ that shows, for the first time in this material, zero resistivity and a shielding fraction of more than 40%. An analysis in the framework of a generalized BCS theory leads to the conclusion that the superconductivity in this system is fully gapped with a possibly non-BCS character. The fully gapped nature qualifies this system as a candidate for a topological superconductor: since this system hosts a topological surface state above T_c [17], depending on whether the parity of the bulk SC state is even or odd, either the surface or the bulk should realize the topological SC state associated with intriguing Majorana edge states.

We acknowledge S. Wada for technical assistance. We thank L. Fu, S. Kuwabata, K. Miyake, and Y. Tanaka for helpful discussions. This work was supported by JSPS (KAKENHI 19674002 and Next-Generation World-Leading Researchers Program), MEXT (Innovative Area "Topological Quantum Phenomena" KAKENHI 22103004), and AFOSR (AOARD 10-4103).

[1] M. Z. Hasan and C. L. Kane, Rev. Mod. Phys. **82**, 3045 (2010).
[2] J. E. Moore, Nature (London) **464**, 194 (2010).
[3] X. L. Qi and S. C. Zhang, arXiv:1008.2026v1.
[4] L. Fu and C. L. Kane, Phys. Rev. Lett. **100**, 096407 (2008).
[5] A. P. Schnyder *et al.*, Phys. Rev. B **78**, 195125 (2008).
[6] X.-L. Qi *et al.*, Phys. Rev. Lett. **102**, 187001 (2009).
[7] X.-L. Qi, T. L. Hughes, and S.-C. Zhang, Phys. Rev. B **81**, 134508 (2010).
[8] J. Linder *et al.*, Phys. Rev. Lett. **104**, 067001 (2010).
[9] M. Sato, Phys. Rev. B **81**, 220504(R) (2010).
[10] L. Fu and C. L. Kane, Phys. Rev. Lett. **102**, 216403 (2009).
[11] A. R. Akhmerov, J. Nilsson, and C. W. J. Beenakker, Phys. Rev. Lett. **102**, 216404 (2009).
[12] Y. Tanaka *et al.*, Phys. Rev. B **79**, 060505(R) (2009).
[13] Y. S. Hor *et al.*, Phys. Rev. Lett. **104**, 057001 (2010).
[14] H. Zhang *et al.*, Nature Phys. **5**, 438 (2009).
[15] Y. Xia *et al.*, Nature Phys. **5**, 398 (2009).
[16] M. L. Cohen, in *Superconductivity*, edited by R. D. Parks (Marcel Dekker, New York, 1969), Vol. 1, Chap. 12.
[17] L. A. Wray *et al.*, Nature Phys. **6**, 855 (2010).
[18] L. Fu and E. Berg, Phys. Rev. Lett. **105**, 097001 (2010).
[19] When Cu substitutes Bi, one $4s$ electron of Cu replaces three $6p$ electrons of Bi to form a σ bond, creating two holes (see Ref. [20]).
[20] A. Vaško *et al.*, Appl. Phys. **5**, 217 (1974).
[21] L. P. Caywood and G. R. Miller, Phys. Rev. B **2**, 3209 (1970).
[22] This midpoint definition for B_{c2} yields a T_c value consistent with the magnetization and specific-heat data.
[23] This shielding fraction becomes 41% if the demagnetization effect [24] is considered.
[24] E. H. Brandt, Phys. Rev. B **60**, 11 939 (1999).
[25] The present situation is actually in between the dirty and clean limits, because we estimate $\xi_0 = \hbar v_F/\pi\Delta_0 = 24$ nm and $\ell = \hbar k_F/(\rho_0 n e^2) = 25$ nm. However, the difference in $1/\lambda^2(T)$ between the two limits is small in the local case; see M. Tinkham, *Introduction to Superconductivity* (McGraw-Hill, New York, 1975), p. 81.
[26] For the calculation of $\lambda_{\rm eff}$, we used the strong-coupling $\Delta(T)$ with $\alpha = 1.9$ consistent with the c_p analysis.
[27] This A_3 gives the Debye temperature $\Theta_{\rm D} = 120$ K.
[28] H. Köhler and H. Fisher, Phys. Status Solidi (b) **69**, 349 (1975).
[29] The contribution of the second conduction band minima (Ref. [28]), whose effective mass is only $\sim 0.1 m_e$, does not significantly alter this conclusion.
[30] J. R. Clem, Physica (Amsterdam) **162C–164C**, 1137 (1989).
[31] H. Padamsee, J. E. Neighbor, and C. A. Shiffman, J. Low Temp. Phys. **12**, 387 (1973).
[32] In a homogeneous nodal superconductor with 100% volume fraction, impurity scattering leads to a finite DOS even at $T = 0$. However, the sample used here consists of SC and non-SC (metallic) parts, and the volume fraction of the latter ($\sim 60\%$) entirely accounts for the observed residual DOS, which is 33% of the total DOS.
[33] We allowed $\gamma_{\rm res}$ and γ_s to be tuned independently.